Spin-polarized transport through an Aharonov–Bohm interferometer embedded with a quantum dot molecule

2009 J. Phys.: Condens. Matter 21 275801

(http://iopscience.iop.org/0953-8984/21/27/275801)

IOP PUBLISHING JOURNAL OF PHYSICS: CONDENSED MATTER

J. Phys.: Condens. Matter **21** (2009) 275801 (5pp) doi:10.1088/0953-8984/21/27/275801

Spin-polarized transport through an Aharonov–Bohm interferometer embedded with a quantum dot molecule

Yibo Ying, Guojun Jin[1] and Yu-qiang Ma

National Laboratory of Solid State Microstructures and Department of Physics, Nanjing University, Nanjing, 210093, People's Republic of China

E-mail: gjin@nju.edu.cn

Received 22 December 2008, in final form 15 May 2009
Published 10 June 2009
Online at stacks.iop.org/JPhysCM/21/275801

Abstract

We propose an Aharonov–Bohm interferometer with a quantum dot molecule embedded in one arm and study the spin-dependent transport due to the interplay of the Fano and Rashba effects. It is found that the Fano resonances of the molecular states exhibit opposite directions of asymmetric tails with one being from peak to dip and the other from dip to peak. The Rashba spin–orbit interaction induces a spin-dependent phase, making the two Fano dips overlap for one spin component of conductance and the two Fano peaks overlap for the other spin component. Both the direction and magnitude of the spin polarization of the conductance are easily controlled and manipulated through the Rashba parameter and interdot coupling strength. In addition, spin accumulations with opposite signs can be generated in the two quantum dots.

In recent years, enormous attention, from both experimental and theoretical physics researchers, has been devoted to the important role played by the spin–orbit (SO) coupling in confined semiconductor heterostructures [1–4]. These structures can be exploited as a means to control and manipulate the spin degree of freedom at the mesoscopic scale useful for phase-coherent spintronic applications. The major problem faced in the spintronic field is that of the generation of spin-polarized carriers and their appropriate manipulation in a controllable environment, preferably in semiconductors. To overcome such obstacles, Datta and Das [5] proposed a spin transistor based on the Rashba SO interaction [6]. Since then, a great deal of theoretical and experimental work has focused on finding a way to control the electron spin with the quantum interference effect, especially as regards the spin-dependent transport in various kinds of ring-type conductors or two path devices [7–10]. This opens up the area of spin-dependent Aharonov–Bohm (AB) physics, including topics such as the Berry phases [11], spin-related conductance modulation [12], spin filters [13, 14] and detectors [15], spin rotation [16], and spin switching mechanisms [17]. Moreover, a quantum dot (QD) can be embedded in one arm of these ring-type structures [18, 19]. The spin degree of freedom in QDs has been an increasingly active subject in the last few years due to its potential applications [20–23], especially in the emerging fields of quantum computation and quantum communication. How to generate and manipulate a spin-resolved current or conductance is the central issue in such applications.

Previous works have dealt with the spin-dependent transport through AB interferometers with one QD or parallel double QDs, for which the interplay of the Fano resonance and Rashba SO coupling provides a remarkable effect [18, 24]. However, the interferometer with serially coupled double QDs, as shown in figure 1, has rarely been addressed, in which the Fano resonance arises from the interference between the states of the QD molecule and the reference arm. Two or three QDs embedded in an AB ring have been realized experimentally [25, 26]. In these two papers, magnetic-field-dependent and gate-voltage-controlled electronic transmissions were studied. The coupling between dots plays an important role in the phase effect or Coulomb blockade effect. Here we will focus our investigation on the spin-polarized transport through an AB ring with two dots embedded in one path. The spin polarization comes from the Rashba SO effect which can be generated by applying a longitudinal electric field. We can find that the coupling between the two dots will affect the spin-polarized transport heavily. For this interferometer, we find that the Fano

[1] Author to whom any correspondence should be addressed.

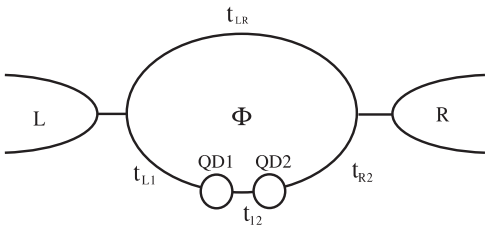

Figure 1. Schematic diagram of an AB ring structure with a two-QD molecule embedded in one arm.

resonances corresponding to the bonding and antibonding molecular states have opposite directions of asymmetric tails. By adjusting the Rashba parameter in the QDs and the magnetic flux penetrating the ring, a large spin filter effect is easily obtained and can even reach 100%. Moreover, tuning the interdot coupling strength can strongly affect the Fano lineshape as well as the spin polarization of conductance, which can be inverted from positive to negative or vice versa. The spin accumulations of the two QDs in the present device are also controllable. We can obtain the up polarization in one QD and the down polarization in the other, which may be of practical use in the storage of quantum information.

The system of a mesoscopic ring with a two-QD molecule can be described by the Hamiltonian

$$\begin{aligned}\mathcal{H} = &\sum_{k\alpha\sigma}\varepsilon_{k\alpha}c^{\dagger}_{k\alpha\sigma}c_{k\alpha\sigma} + \sum_{k\sigma}(t_{\rm LR}{\rm e}^{-{\rm i}\phi}c^{\dagger}_{k{\rm L}\sigma}c_{k{\rm R}\sigma} + {\rm H.c}) \\ &+ \sum_{i\sigma}(\varepsilon_i d^{\dagger}_{i\sigma}d_{i\sigma} + U_i n_{i\sigma}n_{i\bar{\sigma}}) + \sum_{\sigma}(t_{\rm c}d^{\dagger}_{1\sigma}d_{2\sigma} + {\rm H.c}) \\ &+ \sum_{k\sigma}(t_{\rm L1}{\rm e}^{{\rm i}\sigma\varphi}d^{\dagger}_{1\sigma}c_{k{\rm L}\sigma} + t_{\rm R2}{\rm e}^{{\rm i}\sigma\varphi}c^{\dagger}_{k{\rm R}\sigma}d_{2\sigma} + {\rm H.c}). \qquad (1)\end{aligned}$$

Here $c^{\dagger}_{k\alpha\sigma}$ ($c_{k\alpha\sigma}$) and $d^{\dagger}_{i\sigma}$ ($d_{i\sigma}$) are the electron creation (annihilation) operators in lead α ($\alpha = {\rm L}, {\rm R}$) and dot i ($i = 1, 2$) with spin σ, respectively. Each QD includes a single energy level ε_i and intradot Coulomb interaction U_i; the interdot coupling between QD 1 and QD 2 is denoted by $t_{\rm c}$, while the coupling between QD 1 (QD 2) and the left (right) lead is represented by $t_{\rm L1}(t_{\rm R2})$. $t_{\rm LR}$ describes the direct tunneling between the two leads with the AB phase $\phi = 2\pi\Phi/\Phi_0$. Considering that there is the same Rashba SO interaction in the two QDs, an extra phase i $\sigma\varphi$ is added to the hopping terms of $t_{\rm L1}$ and $t_{\rm R2}$.

We now analyze the quantum transport property of this device, through the Keldysh non-equilibrium Green function technique. The charge current flowing from the left lead into the AB ring, contributed by the spin up or spin down electrons, can be derived as [24, 27–29]

$$I_{{\rm L}\sigma} = \frac{2e}{h}\int {\rm d}\varepsilon {\rm Re}\{t_{\rm L1}{\rm e}^{-{\rm i}\sigma\varphi}G^{<}_{1L\sigma}(\varepsilon) + t_{\rm LR}{\rm e}^{-{\rm i}\phi}G^{<}_{{\rm RL}\sigma}(\varepsilon)\}. \qquad (2)$$

The lesser Green functions can be obtained straightforwardly by using the standard Keldysh equation as

$$G^{<}_{\sigma} = G^{\rm r}_{\sigma}g^{{\rm r}-1}_{\sigma}g^{<}_{\sigma}g^{{\rm a}-1}_{\sigma}G^{\rm a}_{\sigma} + G^{\rm r}_{\sigma}\Sigma^{<}_{\sigma}G^{\rm a}_{\sigma}, \qquad (3)$$

where the first and the second terms on the right-hand side describe the elastic and the inelastic transport, respectively. For low temperature and the QDs out of Kondo regime, incoherent processes like sequential tunneling and spin flip cotunneling can be ignored and we only consider the elastic transport which retains the quantum coherence. So we can simply take $\Sigma^{<}_{\sigma} = 0$. $g^{{\rm r}-1}_{\sigma}g^{<}_{\sigma}g^{{\rm a}-1}_{\sigma}$ is diagonal, with the matrix element $g^{{\rm r}-1}_{di\sigma}g^{<}_{di\sigma}g^{{\rm a}-1}_{di\sigma} = 0$ and $g^{{\rm r}-1}_{\alpha\alpha\sigma}g^{<}_{\alpha\alpha\sigma}g^{{\rm a}-1}_{\alpha\alpha\sigma} = 2{\rm i}f_{\alpha}(\varepsilon)/\pi\rho$ ($\alpha = {\rm L}, {\rm R}$), where $f_{\alpha}(\varepsilon) = [{\rm e}^{(\varepsilon-\mu_{\alpha})/k_{\rm B}T} + 1]^{-1}$ is the Fermi distribution function in lead α with chemical potential μ_{α}. Then following the Dyson equation, the retarded (advanced) Green function $G^{\rm r(a)}_{\sigma}$ can be given by $G^{\rm r}_{\sigma} = g^{\rm r}_{\sigma} + g^{\rm r}_{\sigma}\Sigma^{\rm r}_{\sigma}g^{\rm a}_{\sigma}$. The Green function $g^{\rm r}_{\sigma}$ is for the decoupled system (i.e., when $t_{\rm LR} = t_{\rm c} = t_{\rm L1} = t_{\rm R2} = 0$), and in the mean-field approximation its matrix elements are

$$g^{\rm r}_{di\sigma}(\varepsilon) = \frac{\varepsilon - \varepsilon_{di} - U_i + U_i\langle n_{i\bar{\sigma}}\rangle}{(\varepsilon - \varepsilon_{di})(\varepsilon - \varepsilon_{di} - U_i)} \qquad (i = 1, 2) \qquad (4)$$

for the QDs and $g^{\rm r}_{{\rm LL}\sigma}(\varepsilon) = g^{\rm r}_{{\rm RR}\sigma}(\varepsilon) = -{\rm i}\pi\rho$ in the leads. $\langle n_{i\bar{\sigma}}\rangle$ denotes the intradot electron number which can be solved self-consistently by $\langle n_{i\bar{\sigma}}\rangle = -{\rm i}\int({\rm d}\varepsilon/2\pi)G^{<}_{di\bar{\sigma}}(\varepsilon)$. Then by substituting $G^{<}_{1L\sigma}$ and $G^{<}_{{\rm RL}\sigma}$ into equation (2), the current formula can be easily rearranged into the form

$$I_{{\rm L}\sigma} = \frac{2e}{h}\int {\rm d}\varepsilon T_{\sigma}(\varepsilon)[f_{\rm L}(\varepsilon) - f_{\rm R}(\varepsilon)], \qquad (5)$$

in which the transmission coefficient for the symmetric coupling case, $t_{\rm L1} = t_{\rm R2} = t_d$, is

$$T_{\sigma}(\varepsilon) = \Lambda^{-1}(\varepsilon)[(t_{\rm c}\Gamma\cos\tilde{\varphi}_{\sigma} + \pi\lambda t_{\rm LR})^2 + t^2_{\rm c}\Gamma^2\sin^2\tilde{\varphi}_{\sigma}], \qquad (6)$$

with

$$\begin{aligned}\Lambda(\varepsilon) = &|\Gamma^2 - \lambda - 2\pi\Gamma t_{\rm c}t_{\rm LR}\cos\tilde{\varphi}_{\sigma} + \pi^2 t^2_{\rm c}t^2_{\rm LR}|^2 \\ &+ |\Gamma(g^{{\rm r}-1}_{d1\sigma} + g^{{\rm r}-1}_{d2\sigma})|^2,\end{aligned}$$

where we define $\Gamma = \pi\rho|t_d|^2$, $\tilde{\varphi}_{\sigma} = (2\sigma\varphi - \phi)$ and $\lambda = (g^{{\rm r}-1}_{d1\sigma}g^{{\rm r}-1}_{d2\sigma} - t^2_{\rm c})$. In all numerical calculations, we take the coupling strength $t_d = 0.4$ and the density of states in the leads $\rho = 1$, corresponding to a linewidth $2\pi\rho|t_d|^2 \simeq 1$, which is taken as the unit of energy. The chemical potentials of the left and right leads are $\mu_{\rm L} = -\mu_{\rm R} = V/2$ with V as the bias voltage.

For further treatment, we consider that the two single-QD states are coupled and transformed into two new states of a QD molecule [30]. The operators for the molecular states can be expressed as a linear superposition of the QD operators as

$$\begin{pmatrix} f_{+\sigma} \\ f_{-\sigma}\end{pmatrix} = \begin{pmatrix}\cos\beta & -\sin\beta \\ \sin\beta & \cos\beta\end{pmatrix}\begin{pmatrix} d_{1\sigma} \\ d_{2\sigma}\end{pmatrix}, \qquad (7)$$

where $f_{+\sigma}$ and $f_{-\sigma}$ are referred to as the annihilation operators for the bonding and antibonding molecular states and $\beta = (1/2)\tan^{-1}[2t_{\rm c}/(\varepsilon_{1\sigma} - \varepsilon_{2\sigma})]$ with $\varepsilon_{i\sigma} = \varepsilon_i + U\langle n_{i\bar{\sigma}}\rangle$ ($i = 1, 2$) being the effective levels in the mean-field approximation. Thus, the Hamiltonian for the lower arm with the coupled double QDs is diagonalized as

$$\begin{aligned}\tilde{\mathcal{H}} = &\sum_{k\alpha\sigma}(\bar{t}_{\alpha+}c^{\dagger}_{\alpha k\sigma}f_{+\sigma} + \bar{t}_{\alpha-}c^{\dagger}_{\alpha k\sigma}f_{-\sigma} + {\rm H.c}) \\ &+ \sum_{\sigma}(\varepsilon_{+\sigma}f^{\dagger}_{+\sigma}f_{+\sigma} + \varepsilon_{-\sigma}f^{\dagger}_{-\sigma}f_{-\sigma}),\end{aligned}$$

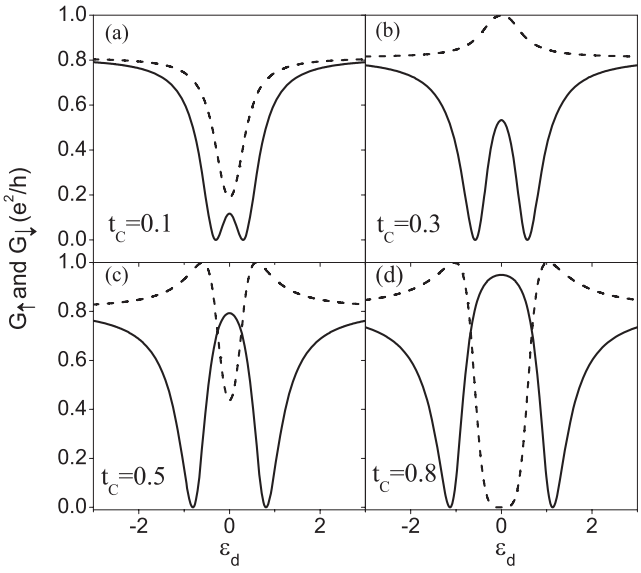

Figure 2. Spin-dependent conductance versus the intradot levels $\varepsilon_1 = \varepsilon_2 = \varepsilon_d$ for different values of the interdot coupling strength. The solid and dashed curves correspond to $G_\downarrow$ and $G_\downarrow$, respectively. Other parameters are $\varphi = \pi/4$, $\phi = \pi/2$, $t_{\rm LR} = 0.2$, $t_d = 0.4$, $U = 0$ and the temperature $T = 0$.

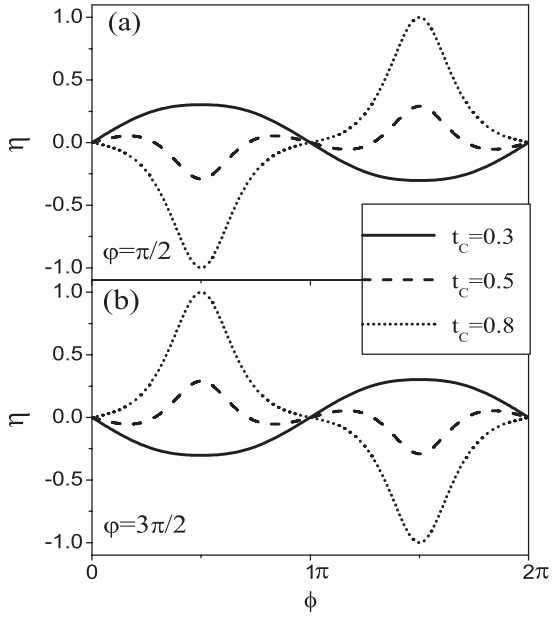

Figure 3. Spin polarization η versus the magnetic flux ϕ for different Rashba parameters: (a) $\varphi = \pi/4$; (b) $\varphi = 3\pi/4$. The solid, dashed, dotted curves correspond to $t_{\rm c} = 0.3, 0.5, 0.8$, respectively. The intradot levels are $\varepsilon_1 = \varepsilon_2 = 0$ with other parameters the same as those in figure 2.

where $\varepsilon_{\pm\sigma} = \frac{1}{2}(\varepsilon_{1\sigma}+\varepsilon_{2\sigma} \pm \sqrt{(\varepsilon_{1\sigma} - \varepsilon_{2\sigma})^2 + 4t_{\rm c}^2})$ are the levels of the molecular states, and the strengths of coupling to the leads are

$$\bar{t}_{\rm L+} = -t_{\rm L1}\cos\beta, \qquad \bar{t}_{\rm R+} = t_{\rm R2}\sin\beta,$$

$$\bar{t}_{\rm L-} = t_{\rm L1}\sin\beta, \qquad \bar{t}_{\rm R-} = t_{\rm R2}\cos\beta.$$

The transmission probability around the bonding or antibonding energy can be approximated by considering the first-order tunneling process as

$$T_{\pm\sigma}(\varepsilon) = \frac{(\xi_\pm + q_{\pm\sigma})^2}{\xi_\pm^2 + 1}|t_{\rm LR}|^2 + \frac{(t_{\rm LR} + q_{\pm\sigma})^2}{\xi_\pm^2 + 1}, \qquad (8)$$

where $\xi_\pm = (\varepsilon - \varepsilon_{\pm\sigma})/\Gamma_\pm$ with $\Gamma_\pm = \pi\rho\sum_\alpha \bar{t}_{\alpha\pm}^2$, and $q_{\pm\sigma} = \bar{t}_{\rm L\pm}\bar{t}_{\rm R\pm}\cos(2\sigma\varphi - \phi)/\Gamma_\pm$ is the Fano parameter which determines the asymmetry of the Fano lineshape. It is found that $\bar{t}_{\rm L+}\bar{t}_{\rm R+} = -\bar{t}_{\rm L-}\bar{t}_{\rm R-}$; therefore the Fano asymmetric parameters corresponding to the bonding and antibonding states have the relationship

$$q_{+\sigma} \times q_{-\sigma} < 0,$$

which means that their Fano resonances have opposite asymmetries (one is from a peak to a dip and the other is from a dip to a peak or vice versa). Thus, one can expect the evolution of lineshape for the transmission to be peak → dip → dip → peak (PDDP) or dip → peak → peak → dip (DPPD), which can be controlled by the Rashba interaction through $\cos(2\sigma\varphi - \phi)$ in $q_{\pm\sigma}$.

To demonstrate the asymmetry of the Fano lineshape, we show the linear conductance $G_\sigma = \frac{e^2}{h}T_{\pm\sigma}(\varepsilon)$ as a function of dot levels with the Rashba SO interaction $\varphi = \pi/4$ and the reduced flux $\phi = \pi/2$ in figure 2. The interference between the channel through the bonding (antibonding) molecular state and the reference arm give rise to the Fano effect. The overlap of the Fano resonances with opposite directions of asymmetric tails can obviously be seen and the existence of the Rashba SO interaction split the two spin components of conductance as indicated by $q_{\pm\sigma} \propto \cos(2\sigma\varphi - \phi)$. It is also interesting to note that the Fano effect can be strongly affected by the interdot coupling strength. Increasing $t_{\rm c}$ from $t_{\rm c} = 0.1$ in figure 2(a) to $t_{\rm c} = 0.3$ in figure 2(b), the conductance curve for the spin up electron evolves from one dip structure to one peak while the spin down conductance was retained with the PDDP structure. Increasing $t_{\rm c}$ further, in figure 2(c) $t_{\rm c} = 0.5$ and figure 2(d) $t_{\rm c} = 0.8$, the Fano resonance for spin down electron rises again with the characteristic of DPPD and the Fano resonance for spin up electron changes into the form of PDDP. For even larger $t_{\rm c}$, the characteristics of the Fano resonances for the two spin components remain unchanged.

It can be found that the spin filter effect is greatly enhanced when the interdot coupling increases. Figure 3 shows the spin polarization $\eta = (G_\uparrow - G_\downarrow)/(G_\uparrow + G_\downarrow)$ versus the magnetic flux for three values of $t_{\rm c} = 0.3, 0.5, 0.8$ in the case of zero-bias voltage. It is noteworthy that the spin polarization is inverted from small positive to large negative by increasing $t_{\rm c}$ or vice versa. The magnitude of the spin polarization reaches 100% when $t_{\rm c} = 0.8$. By comparing $\varphi = \pi/4$ in figure 3(a) with $\varphi = 3\pi/4$ in figure 3(b), one can see that the direction of spin polarization gets reversed by tuning the Rashba SO interaction. So in the present device both the direction of spin polarization and its magnitude are easily controllable by changing the system parameters, which are experimentally accessible.

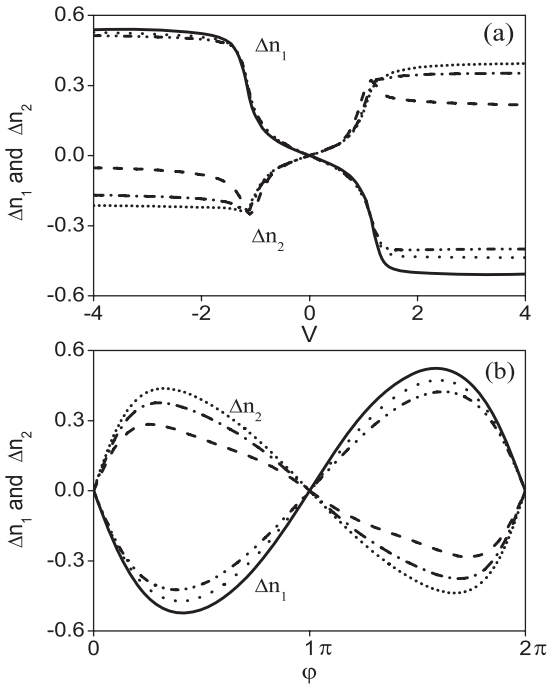

Figure 4. Spin accumulation. (a) Δn_1 (solid, dotted, and dash–dot–dotted lines for $U = 3$, 6, and 9, respectively) and Δn_2 (dashed, dash–dotted, and short dotted lines for $U = 3$, 6, and 9, respectively) versus the bias V for $\varphi = \pi/4$. (b) Δn_1 and Δn_2 versus φ for different intradot Coulomb interactions U at $V = 3.0$. The other parameters are $t_{\rm LR} = 0.4$, $t_{\rm c} = 0.8$ and the intradot levels $\varepsilon_1 = -\varepsilon_2 = 0.25$.

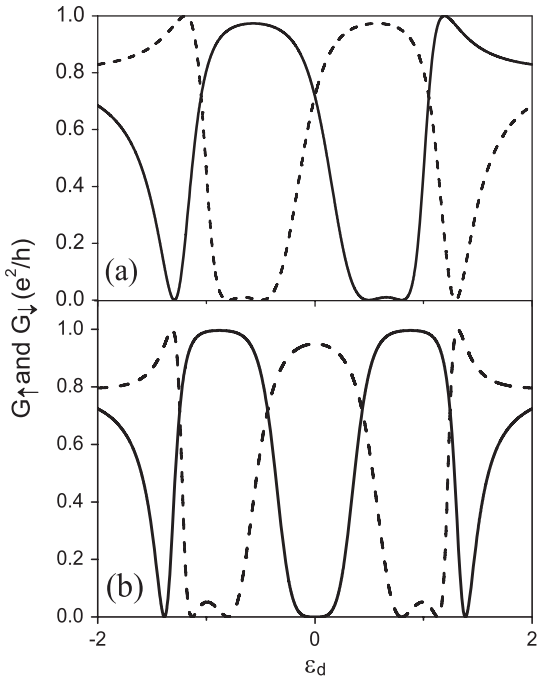

Figure 5. Spin-dependent conductance versus the intradot level for different numbers of QDs in the molecule: (a) three QDs; (b) four QDs. The solid, dashed curves correspond to spin down and spin up, respectively. The other parameters are the same as those for figure 2.

We can also investigate the spin accumulations Δn_i ($\Delta n_i = n_{i\uparrow} - n_{i\downarrow}$) in the two QDs when the bias voltage is nonzero. The total effective strengths of coupling between the QD 1 and the left and right leads are

$$T_{\mathrm{L}1\sigma} = |t_{\mathrm{L}1}\mathrm{e}^{\mathrm{i}\sigma\varphi} + t_{\mathrm{c}} g^r_{d2\sigma} t_{\mathrm{R}2}(-i\pi\rho) t_{\mathrm{LR}}\mathrm{e}^{-\mathrm{i}\sigma\varphi}|$$
$$= |t_{\mathrm{L}1}|^2 + |\tilde{t} g^r_{d2\sigma}|^2 + 2t_{\mathrm{L}1} g^r_{d2\sigma}\tilde{t}\sin(2\sigma\varphi), \quad (9)$$

$$T_{\mathrm{R}1\sigma} = |t_{\mathrm{R}2} g^r_{d2\sigma} t_{12}\mathrm{e}^{-\mathrm{i}\sigma\varphi} + t_{\mathrm{L}1}(-i\pi\rho) t_{\mathrm{LR}}\mathrm{e}^{\mathrm{i}\sigma\varphi}|$$
$$= |t_{\mathrm{L}1}\pi\rho t_{\mathrm{LR}}|^2 + |t_{\mathrm{c}} t_{\mathrm{R}2} g^r_{d2\sigma}|^2 - 2t_{\mathrm{L}1} g^r_{d2\sigma}\tilde{t}\sin(2\sigma\varphi), \quad (10)$$

where $\tilde{t} = \pi\rho t_{\mathrm{c}} t_{\mathrm{R}2} t_{\mathrm{LR}}$, and $g^r_{d2\sigma}$ is expressed by equation (4). In the same way, we can obtain the strengths of coupling between QD 2 and the two leads. The spin-dependent coupling strengths make it easier for one spin to inject into a QD but harder for it to leave, while for the other spin it is harder to inject but easier to leave, giving rise to spin accumulation in the two QDs. In figure 4(a), we show the spin accumulations of the two QDs versus the bias voltage, which have the following features: (1) the spin accumulations can be generated without magnetic field when the bias is nonzero. (2) Δn_1 and Δn_2 can have opposite signs for properly chosen intradot levels. (3) Both Δn_1 and Δn_2 reverse their signs when the bias voltage is tuned from $V < 0$ to $V > 0$ and the magnitude of the spin accumulation increases with V. One can find that the spin accumulation is affected by the Rashba interaction. In figure 4(b), both Δn_1 and Δn_2 versus φ exhibit a periodic function with a period of 2π. $|\Delta n_2|$ increases with U; in contrast, $|\Delta n_1|$ decreases when U increases, which can also be seen in figure 4(a).

As an extension, we can also discuss the cases of a three-QD molecule and a four-QD molecule embedded in a ring arm. For simplicity, we assume that each QD has the same level position ε_d and the direct tunnel coupling strengths, for between adjacent QDs, are taken to be equal as $t_{\rm c} = 0.8$. The effective molecular states can be obtained in the same way as for the two-QD case. It is interesting to find that the overlap of Fano dips or Fano peaks also exists and the conductance shows nearly periodic behavior as a function of the QD level when the number of QD increases, as can be seen in figure 5. Furthermore, the spin polarization is tunable through the QD number and it is also periodic with the QD level when the Rashba SO interaction exists between lead and its adjacent QD.

In conclusion, we have investigated the spin-polarized conductance in a two-terminal AB ring device that contains two serial QDs in one arm. The two directly coupled quantum dots form bonding and antibonding molecular states and the corresponding Fano resonances have asymmetric tails with opposite directions, which overlap to give rise to a large spin filter effect when the Rashba SO interaction exists. Compared to the AB ring with one QD, the present device with a two-QD molecule in one arm of the AB ring utilizes the Fano effect corresponding to a molecular state. The unique phenomenon of overlap of two asymmetric Fano resonances, lacking in the one-QD ring, efficiently enhances the spin filter effect. In addition, the interdot coupling provides an additional tuning parameter which drastically modulates the spin polarization. It should also be pointed out that the spin filter effect of the present device is much more efficient than the parallel double-QD ring [18], in which the spin filter effect is due to the interference between the bonding molecular state and

the antibonding molecular state, whereas, in our device, the interference between the reference arm and two molecular states dominates, and shows the characteristics of tuning the Fano resonances by interdot coupling and Rashba interaction not seen in the parallel double-QD ring. Thus the spin-polarized conductance is readily realized by adjusting the interdot coupling and the Rashba parameter. There is an another advantage of the present device: that the Rashba effect can induce spin accumulation in the two QDs with one being up polarized and the other down polarized, which may be of practical use in quantum information storage.

Acknowledgments

This work was supported by the National Natural Science Foundation (Grant Nos 10674058, 60876065) and the State Key Program for Basic Research (Grant Nos 2006CB921803, 2009CB929504) of China.

References

[1] Nitta J, Meijer F E and Takayanagi H 1999 *Appl. Phys. Lett.* **75** 695
[2] Frustaglia D, Hentschel M and Richter K 2004 *Phys. Rev.* B **69** 155327
[3] Molnár B, Peeters F M and Vasilopoulos P 2004 *Phys. Rev.* B **69** 155335
[4] Capozza R, Giuliano D, Lucignano P and Tagliacozzo A 2005 *Phys. Rev. Lett.* **95** 226803
[5] Datta S and Das B 1990 *Appl. Phys. Lett.* **56** 665
[6] Rashba E I 1960 *Fiz. Tverd. Tela* **2** 1224
Rashba E I 1960 *Sov. Phys.—Solid State* **2** 1109 (Engl. Transl.)
Bychkov Y A and Rashba E I 1984 *J. Phys. C: Solid State Phys.* **17** 6039
[7] Souma S and Nikolić B K 2004 *Phys. Rev.* B **70** 195346
[8] Wu B H and Cao J C 2006 *Phys. Rev.* B **74** 115313
[9] Cohen G, Hod O and Rabani E 2007 *Phys. Rev.* B **76** 235120
[10] Sheng J S and Chang K 2006 *Phys. Rev.* B **74** 235315
[11] Aronov A G and Lyanda-Geller Y B 1993 *Phys. Rev. Lett.* **70** 343
[12] Shelykh I A, Bagraev N T, Galkin N G and Klyachkin L E 2005 *Phys. Rev.* B **71** 113311
[13] Citro R, Romeo F and Marinaro M 2006 *Phys. Rev.* B **74** 115329
[14] Wu S, Jin G and Ma Y 2007 *J. Phys.: Condens. Matter* **19** 436212
[15] Ionicioiu R and D'Amico I 2003 *Phys. Rev.* B **67** 041307(R)
[16] Mal'shukov A G, Shlyapin V V and Chao K A 2002 *Phys. Rev.* B **66** 081311(R)
[17] Frustaglia D, Hentschel M and Richter K 2001 *Phys. Rev. Lett.* **87** 256602
[18] Chi F, Liu J and Sun L 2007 *J. Appl. Phys.* **101** 093704
[19] Gong W, Zheng Y and Lü T 2006 *Appl. Phys. Lett.* **92** 042104
[20] Tsymbal E Y, Mryasov O N and LeClair P R 2003 *J. Phys.: Condens. Matter* **15** R109
[21] Žutić I, Fabian J and Das Sarma S 2004 *Rev. Mod. Phys.* **76** 323
[22] Li S S, Abliz A, Yang F H, Niu Z C, Lin F S, Xia J B and Hirose K 2002 *J. Appl. Phys.* **92** 6662
[23] Li S S, Chang K, Xia J B and Hirose K 2003 *Phys. Rev.* B **68** 245306
[24] Sun Q F, Wang J and Guo H 2005 *Phys. Rev.* B **71** 165310
[25] Mühle A, Wegscheider W and Haug R J 2008 *Appl. Phys. Lett.* **92** 013126
[26] Sigrist M, Fuhrer A, Ihn T, Ensslin K, Ulloa S E, Wegscheider W and Bichler M 2004 *Phys. Rev. Lett.* **93** 066802
[27] Meir Y and Wingreen N S 1992 *Phys. Rev. Lett.* **68** 2512
[28] Jauho A, Wingreen N S and Meir Y 1994 *Phys. Rev.* B **50** 5528
[29] Bulka B R and Stefański P 2001 *Phys. Rev. Lett.* **86** 5128
[30] Lu H, Lü R and Zhu B 2005 *Phys. Rev.* B **71** 235320